

## Abstract

It has recently become possible to record electroencephalography (EEG) and the blood-oxygen level dependent (BOLD) contrast signal (Figure 4) used in functional magnetic resonance imaging (fMRI) simultaneously in human subjects [1].

While EEG remains an essential tool in cognitive neuroscience and clinical practice, its spatial localization capabilities are poor. Neuroimaging using fMRI-BOLD is capable of providing good spatial resolution, but its temporal scale is much slower than the brain's electrophysiological activity.

Very few studies have attempted to address the critical problem of fully integrating EEG and BOLD [2,3,4], which, if successful, would lead to a better understanding of the neural processes that underlie both signals, and non-invasive methods for the assessment of cognitive function.

Based on our working hypothesis that very low frequency oscillations ( $\leq 0.166$  Hz) common to both EEG and BOLD signals can be used to link the spatiotemporal information contained in each signal [5], we investigate the neural state changes accompanying normal human descent into Stage 2 sleep using a variety of linear and nonlinear measures, particularly the demodulation of low frequency envelopes from EEG data [6] (Figures 1,2), and stochastic phase synchronization [7].

Figure 1: EEG-Demodulated Slow Wave Envelope, Example Result

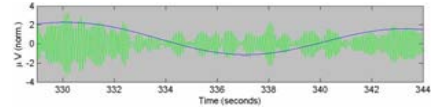


Figure 2: LVIS EEG Demodulated Slow Wave Envelope - Awake Subject

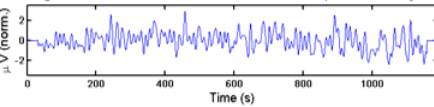


Figure 3: Regions of Interest

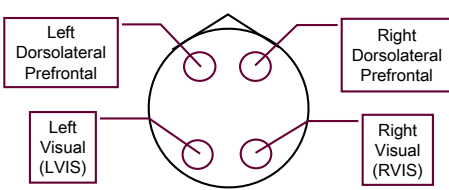


Figure 4: LVIS fMRI Time Series - Awake Subject

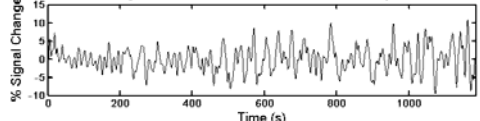
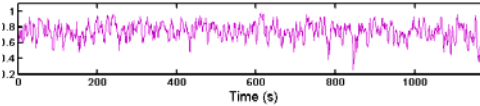


Figure 5: Synchronization Index Time Series Between LVIS Channels O1 & P1



## Stochastic Phase Synchronization

Both EEG electrode recordings and summations of fMRI voxels in particular regions of interest (Figure 3) can be reduced to simple time series for data analysis. Each time series can be looked at as an analytic signal,

$$\psi(t) = s(t) + i\bar{s}(t) = A(t)e^{i\phi(t)}$$

where the Hilbert transform  $\bar{s}(t)$  of  $s(t)$  is given by

$$\bar{s}(t) = \frac{1}{\pi} P.V. \int_{-\infty}^{\infty} \frac{s(\tau)}{t-\tau} d\tau$$

(P.V. in this equation means that the integral is taken with regard to the Cauchy principal value). The instantaneous phase  $\phi(t)$  appearing in the analytic signal may be extracted and interpreted as the instantaneous phase for the EEG or fMRI time series. The instantaneous phase differences,  $\Phi_{nm}(t)$ , between the phases of two series can then be calculated. If the phase locking condition

$$|n\phi_1(t) - m\phi_2(t)| = |\Phi_{nm}(t)| < \text{const}$$

is satisfied for any integers  $n$  and  $m$ , then the channels are said to be  $n:m$  phase locked. Once the phase locking condition is met and the instantaneous phase differences are calculated, the normalized cyclic relative phase [8] distribution  $\Phi_{nm} = \Phi_{nm} \bmod 2\pi$  is calculated, and may be represented in a histogram format. A sharp peak in this cyclic relative phase distribution indicates a preferred phase difference between two signals, upon which a claim for statistical synchronization between them may be based. The intensity of the first Fourier mode of the distribution,

$$\gamma^2 = (\cos\langle\phi(t_i)\rangle)^2 + (\sin\langle\phi(t_i)\rangle)^2$$

with  $\langle \rangle$  denoting a time average, defines the synchronization index  $\gamma$ , which varies from 0 to 1 and defines the quality of synchronization between the two channels.

In addition, when working with EEG data collected at a relatively high sampling rate, a sliding time window analysis can be performed in order to calculate the synchronization index  $\gamma$  as a function of time between two signals [8] (Figure 5).

## Mathematical Model of Demodulation

Our method for extracting low-frequency envelopes from EEG data is analogous to the method used in AM radio. The model for a transmitted AM signal is given by

$$x(t) = A_c [1 + m s(t)] \cos(2\pi f_c t + \phi)$$

where  $s(t):|s(t)| < 1$  is the (low-frequency) signal to be transmitted,  $m:0 < m < 1$  is the modulation index,  $f_c$  is the frequency of the carrier wave in Hertz,  $\phi:0 \leq \phi < 2\pi$  is the (usually unknown) phase of the carrier wave,  $A_c:A_c > 0$  is the strength of the signal, and  $x(t)$  is the transmitted signal. The signal  $s(t)$  must be band limited so that its Fourier transform,  $S(f)$ , is equal to 0 for  $|f| > B_s$ , where  $2B < f_c$ .

The inverse problem is to recover  $s(t)$  from  $x(t)$ . Because the phase,  $\phi$ , is unknown, noncoherent demodulation methods are usually used. The first step of the method we employed to prepare the preliminary data was to compute the magnitude of each sample of  $x(t)$ . The output of this full-wave rectifier is

$$z(t) = |x(t)| = A_c [1 + m s(t)] |\cos(2\pi f_c t)|$$

The Fourier series for  $z(t)$  is given by

$$z(t) = \frac{2A_c}{\pi} [1 + m s(t)] + \frac{4A_c}{\pi} [1 + m s(t)] \sum_{n=1}^{\infty} \frac{(-1)^n}{4n^2 - 1} \cos 2\pi(2n) f_c t$$

All of the terms except the first one are centered at multiples of the carrier frequency,  $f_c$ , which implies that if  $f_s > 2B_s$ , then low-pass filtering  $z(t)$  separates the term  $2A_c [1 + m s(t)]/\pi$  from the other terms. Then the original signal,  $s(t)$ , is recovered by blocking the DC component, i.e., subtracting the mean [6].

The equations given above assume a perfect modulator, given by  $\cos(2\pi f_c t)$ , which has the Fourier transform  $(1/2)[\delta(f - f_c) + \delta(f + f_c)]$ . The demodulation method still works if the modulation is with a high-frequency function other than a sinusoid. Then a version of  $s(t)$  is still recovered, but it is smoothed by convolution with the Fourier transform of the modulation function.

## Results 1

As part of our preprocessing algorithm, all EEG data was referenced to the average reference, and band-pass filtered into classically defined frequency bands: delta (1-4 Hz), theta (4-8 Hz), and alpha (8-12 Hz). The alpha band is of particular interest for our study as several labs have reported changes in its spectral power to be correlated with visual stimulus [9]. Additionally, alpha oscillations are known to wane during sleep.

By means of the Hilbert Transform (below), we calculated the instantaneous phases of EEG Slow Wave Envelope time series and BOLD time series. We observed that a 0.1 Hz envelope most closely matched the BOLD time series in total number of oscillations. Therefore, using these 0.1 Hz EEG envelopes, signature channels from each region of interest (Figure 3) were averaged to produce a wave representing the general neural response of the region (Figure 2). Then, we calculated the synchronization index (above) between Left Visual BOLD time series and every region's EEG envelope response, looking for differences between wake and sleep.

LVIS fMRI with LVIS EEG Envelopes			RVIS fMRI with RVIS EEG Envelopes		
Subject	$\gamma_0$	State	Subject	$\gamma_0$	State
1	0.112	awake	1	0.082	awake
2	0.187	awake	2	0.185	awake
3	0.213	awake	3	0.215	awake
4	0.230	awake	4	0.234	awake
5	0.244	awake	5	0.306	awake
6	0.085	sleep	6	0.038	sleep
7	0.105	sleep	7	0.097	sleep
8	0.117	sleep	8	0.106	sleep
9	0.129	sleep	9	0.128	sleep
t-test 0.016			t-test 0.035		

The results of the two-tailed, two-sample, unequal variance t-test show that the synchronization between Left Visual fMRI BOLD signals and alpha band EEG envelopes is distinctly higher when a subject is awake versus when they are asleep, as one might expect. However, other fMRI regions of interest did not pass the t-test, including Right Visual fMRI.

As a second experiment, we tested the synchronization and linear cross-correlation region-to-region between EEG envelopes with other EEG envelopes, and then fMRI BOLD with other fMRI BOLD, in order to determine whether regional pairs of higher synchronization/correlation in EEG coincided with regional pairs of higher synchronization/correlation in fMRI. We found that both the synchronization and also the cross-correlation between EEG envelope time series pairs was always much higher than synchronization/correlation between fMRI BOLD time series pairs (average  $\geq 0.045$  for alpha data).

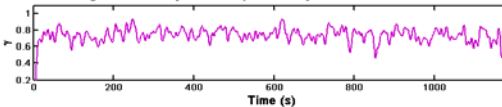
## Hemodynamic Response

The linear transform model of fMRI suggests that fMRI response to any pattern of neural activity can be predicted by convolving the time course of the neural activity (in this case, EEG data, or additionally, the synchronization index between two regions of interest as a function of time) with a shift-invariant linear temporal filter [10] (Figure 6). This filter is modeled after a gamma function,

$$h(t) = \frac{(t/\tau)^{n-1} e^{-t/\tau}}{\tau(n-1)!}$$

where  $t$  is time,  $\tau$  is the time constant for the function's rise and fall, and  $n$  represents a phase delay.

Figure 6: Hemodynamic Response of Synchronization Time Series



## Results 2

The measured potential at a given electrode is thought to represent the collective activity of a large population of neurons. Our next hypothesis was that if different electrodes in the same region of interest show synchronization at a particular time, then many large groups of neurons would be firing in unison at this time, and this communal activity might show up as a rise in the BOLD signal.

The synchronization index was calculated across sliding windows 3 - 6 seconds in length, using various intervals between adjacent windows. (Figure 5) We were careful to allow at least 30 oscillations in the EEG signal to produce a robust result, yielding the same synchronization time series for every combination of parameters.

We observed that the synchronization time series calculated using this method fluctuates on time scales very comparable to the BOLD signal (Figure 7). The synchronization index time series can also be convolved with the hemodynamic response function (above) [11], and this waveform also contains power spectral density content resembling that of fMRI (Figure 8).

Secondly, cross-correlation between these synchronization time series and the BOLD response from the same regions of interest have shown peak values slightly higher than 0.20. However even if correlations did exist between these time series, one would not necessarily expect them to be large, given the slow physiological nature of the BOLD response and the high degree of nonlinearity in biological systems.

Figure 7

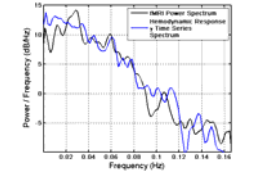
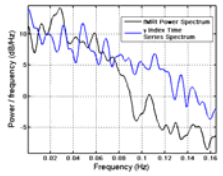


Figure 8



## Conclusions

- EEG Slow Wave Envelopes correlated/synchronized with the fMRI BOLD signal from particular regions of interest have not (yet) provided a clear enough distinction between quiet resting wake and Stage 2 sleep. Nor has the combination provided an assumed link between the spatial and temporal information contained in each modality.
- However, many factors may have contributed to this result. For instance, quietly resting subjects could be drowsy, and Stage 2 sleep is not a very deep sleep stage. The neurological patterns in these protocols may not be distinctly different from outset. Further experiments (planned) with deeper sleep stages and visually evoked potentials might provide a better comparison.
- There are measures of EEG time series which change over time at frequencies very relevant to BOLD imaging (Figures 7,8). There are also methods, i.e. convolution with the hemodynamic response function (above, Figure 6), which may relate these neurological measurements to BOLD activation.

## References

- [1] R. Goldman, J. Stern, J. Engel, J., M.S. Cohen (2002) Simultaneous EEG and fMRI of the alpha rhythm. *Neuroreport* 13:2487-2492.
- [2] V.D. Calhoun, T. Adali, G.C. Prattish, K.A. Kuhl (2005) Neural chronometry of target detection: Fusion of hemodynamic and event-related potential data. *NeuroImage* 30:244-263.
- [3] S. Debener, M. Ullsperger, M. Siegel, K. Fritzer, D.V. von Cramon, A.K. Engel (2005) The alpha rhythm: A window of concentration electroencephalogram and functional magnetic resonance imaging identifies the dynamics of performance monitoring. *NeuroImage* 27:1212-1219.
- [4] T. Eschke, K. Specht, M. Moosmann, M. Müller, J. Jung, R. Quaresima, H. Hoyer, K. Hugdahl (2005) Assessing the spatiotemporal evolution of neuronal activation with single-fMRI voxel-related potentials and functional MRI. *Phys. Rev. E* 72:011907.
- [5] D.A. Leopold, J. Murayama, M.K. Logothetis (2003) Very slow activity fluctuations in monkey visual cortex: Implications for functional brain imaging. *Cerebral Cortex* 13:422-433.
- [6] H. Stark, P.B. Tuter (1978) Modern Electrical Communications Theory and Systems. Prentice-Hall, Inc. Englewood Cliffs, New Jersey.
- [7] M.C. Rosenblum, A.S. Pikovsky, J. Kurths (1996) Phase synchronization of chaotic oscillators. *Phys. Rev. Lett.* 76(11):1804-1807.
- [8] P. Tass, M.C. Rosenblum, J. Weule, J. Kurths, A. Pikovsky, J. Volkman, A. Schmalzer, H.J. Freund (1998) Detection of nonphase locking from noisy data: application to Magnetoencephalography. *Phys. Rev. Lett.* 81(15):3291-3294.
- [9] W. Klimesch (1999) EEG alpha and theta oscillations reflect cognitive and memory performance: a review and analysis. *Brain Res. Rev.* 29:151-176.
- [10] G.M. Boynton, S.A. Engel, G.H. Glover, D.J. Heeger (1996) Linear systems analysis of functional magnetic resonance imaging in human V1. *J. Neurosci.* 16(13):4207-4221.
- [11] H. Mizuhara, Y. Yamaguchi (2007) Human cortical circuits for central executive function emerge by theta phase synchronization. *NeuroImage* 38:232-244.